Shock compaction of cubic boron nitride powders

TAMOTSU AKASHI
Center for Explosives Technology Research, New Mexico Institute of Mining and Technology, Socorro, New Mexico 87801, USA

AKIRA B. SAWAOKA
Research Laboratory of Engineering Materials, Tokyo Institute of Technology, Yokohama 227, Japan

C-BN powders with different grain sizes were dynamically compacted by explosive shock loading using approximate peak pressures from 33 to 77 GPa. The density and the microhardness of the resulting c-BN compacts were strongly dependent upon the grain size of the c-BN powders used as the starting materials. The best c-BN compacts, with 98% of the theoretical density and microhardness of 51.3 GPa, were obtained from the coarse c-BN powder (40 to 60 μm). In the compacted fine c-BN powder (2 to 4 μm) conversion of the c-BN to low density forms of BN at a residual temperature degraded the interparticle bonding significantly. X-ray line-broadening analysis of the compacted c-BN powders indicated that the residual lattice strain increased with the increase in grain size of the starting powder, while the crystallite size was independent of the grain size.

1. Introduction

Chemical and physical properties of cubic boron nitride (c-BN) are very similar to those of a diamond [1]. Polycrystalline c-BN compact can be expected to have good toughness (superior to single crystal c-BN) in addition to high hardness, analogous to natural polycrystalline diamond, carbonardo. However, c-BN and diamond are typically hard-to-sinter materials, even when high-temperature and high-pressure techniques are used, due to their strong covalent bonding and their stability at high temperatures and pressures [2–4].

Shock compaction is one of the powder compaction processes and seems to have considerable potential in the fabrication of c-BN and diamond powders as well as in the densification. In the shock-compaction process, powder compact can be densified to near the theoretical density at the shock front with subsequent interparticle bonding. The effects of shock compression on powder materials depend strongly upon the nature of the chemical bonding of the materials and their physical properties [5, 6]. Thus, the required shock-compaction conditions are also dependent upon the chemical and physical properties as well as the characteristics of the powders [7, 8]. In addition, in the shock consolidation of c-BN powder, the zinc blende type structure should be preserved through the shock-compaction process in order to develop good mechanical properties.

In this work, c-BN powders with different grain sizes were dynamically compacted to study the effects of grain size on the densification and consolidation processes under the shock-loading conditions.

2. Experimental procedures

2.1. Starting materials

Commercial-grade c-BN powders with different grain sizes were used as the starting materials. Three sizes were used: 2 to 4 μm grade (Showa Denko Co. Ltd.) and 10 to 20 μm and 40 to 60 μm grade (General Electric Co. Ltd.). Scanning electron micrographs of the as-received c-BN powders are shown in Fig. 1. The powders were composed of angular particles as seen in Fig. 1. A spectrochemical analysis of the impurities in the starting c-BN powders is listed in Table I. The powders without additives were cold-pressed to form discs 5 mm thick and 12 mm in diameter with a density of 60% of the theoretical density in stainless steel capsules [7] and then shock-compressed.

2.2. Shock compaction experiments

Shock treatments were carried out using a mouse-trap type plane-wave generator and a momentum-trap recovery system. Details of the shock-treatment fixture have been reported elsewhere [7]. The impact velocity employed in this work was 2.1 km sec^{-1}. The shock pressures induced in the c-BN powder compacts were approximated from the calculation for titanium

TABLE I Spectrochemical analysis of starting c-BN powders

2 to 4 μm grade c-BN		10 to 20 μm grade c-BN		40 to 60 μm grade c-BN	
Element	Weight (p.p.m.)	Element	Weight (p.p.m.)	Element	Weight (p.p.m.)
Si	800	Si	800	Si	800
Mg	100	Ca	5	Ca	5
Mn	10	Mg	1	Mg	1
Fe, Cr	< 1	Fe	< 1	Fe	< 1
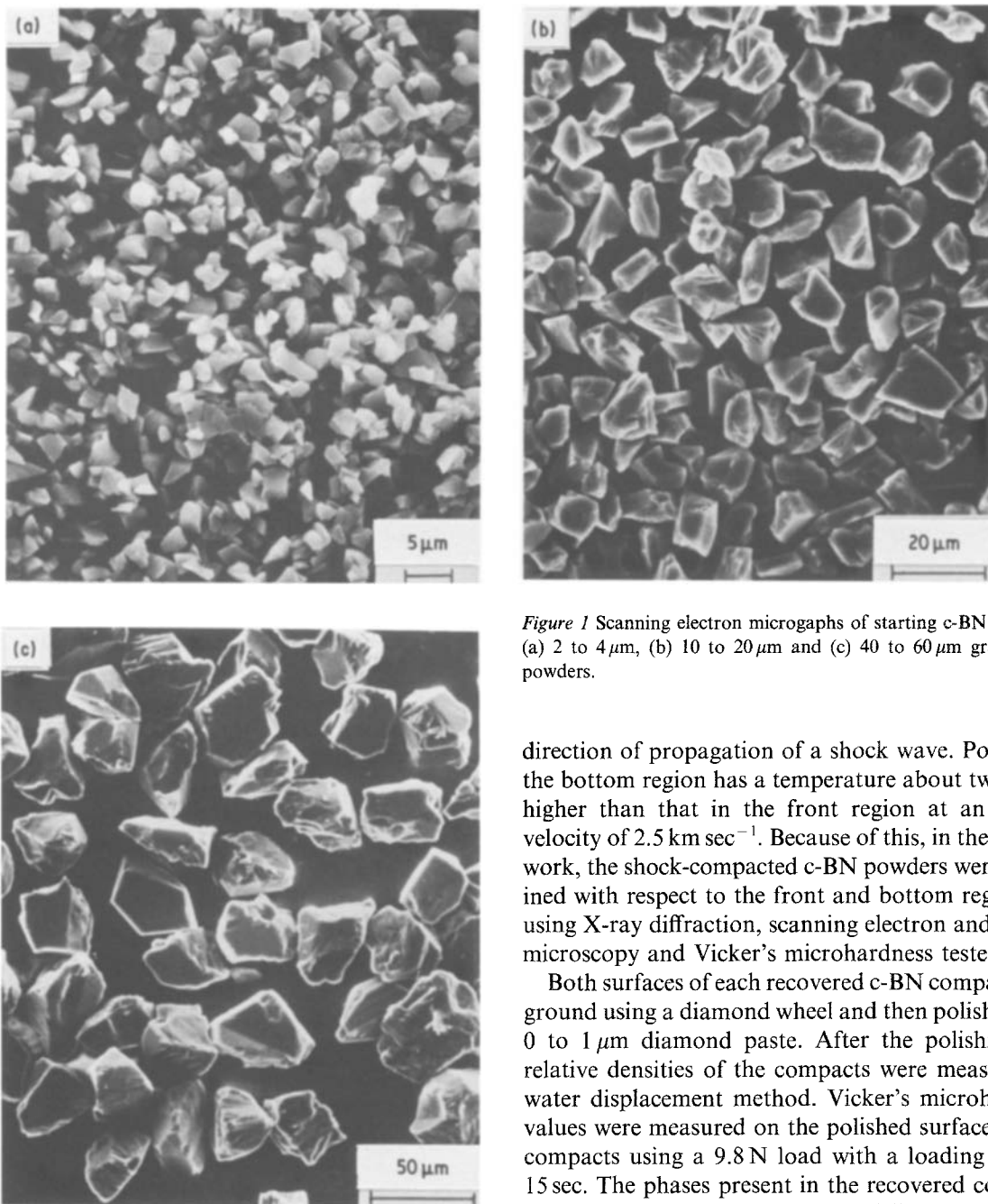
Figure 1 Scanning electron microgaphs of starting c-BN powders. (a) 2 to 4 μm, (b) 10 to 20 μm and (c) 40 to 60 μm grade c-BN powders.

dioxide (rutile type) powder at an impact velocity of 2.5 km sec^{-1} [9]. The peak pressures obtained by scaling the pressures in [9] according to the impact velocity of 2.1 km sec^{-1} were 33 and 75 GPa for the outer and centre regions within the powder compact, respectively. Immediately after impact, fixtures containing the capsules were plunged into a water basin and quickly cooled before being recovered. After the shock treatments, c-BN samples were carefully taken out of the capsules using a lathe.

2.3. Characterization of compacted c-BN powders

The computer calculations using CSQ code [9] show that in the present shock-treatment fixture, the pressure and the temperature induced by shock loading depend strongly upon the position within the powder compact. Most noticeably, shock temperatures in the front and bottom regions at a given impact velocity differ significantly. These positions correspond to the direction of propagation of a shock wave. Powder in the bottom region has a temperature about two times higher than that in the front region at an impact velocity of 2.5 km sec^{-1}. Because of this, in the present work, the shock-compacted c-BN powders were examined with respect to the front and bottom regions by using X-ray diffraction, scanning electron and optical microscopy and Vicker's microhardness tester.

Both surfaces of each recovered c-BN compact were ground using a diamond wheel and then polished with 0 to 1 μm diamond paste. After the polishing, the relative densities of the compacts were measured by water displacement method. Vicker's microhardness values were measured on the polished surfaces of the compacts using a 9.8 N load with a loading time of 15 sec. The phases present in the recovered compacts were examined using an X-ray diffractometer with Ni-filtered Cu$K\alpha$ radiation. The residual lattice strain and the crystallite size of the compacted c-BN powders were determined by X-ray line-broadening analysis using the Hall equation [10] referring to well annealed alumina powder. X-ray diffraction patterns for the phase indentification and the line-broadening analysis were also taken on the polished surfaces of the compacts. Microstructures of the fracture and polished surfaces of the compacted c-BN samples were observed by a scanning electron and optical microscopy.

3. Results and discussion

C-BN compacts were recovered as a whole disc containing several cracks. The difference in the cracking behaviours of the front and bottom surfaces of the compacts was due to the difference in their pressure and temperature histories within the powder compacts during and after shock compression. Fig. 2 shows such crack generation in the compacted c-BN sample obtained from 40 to 60 μm grade powder. Photographs
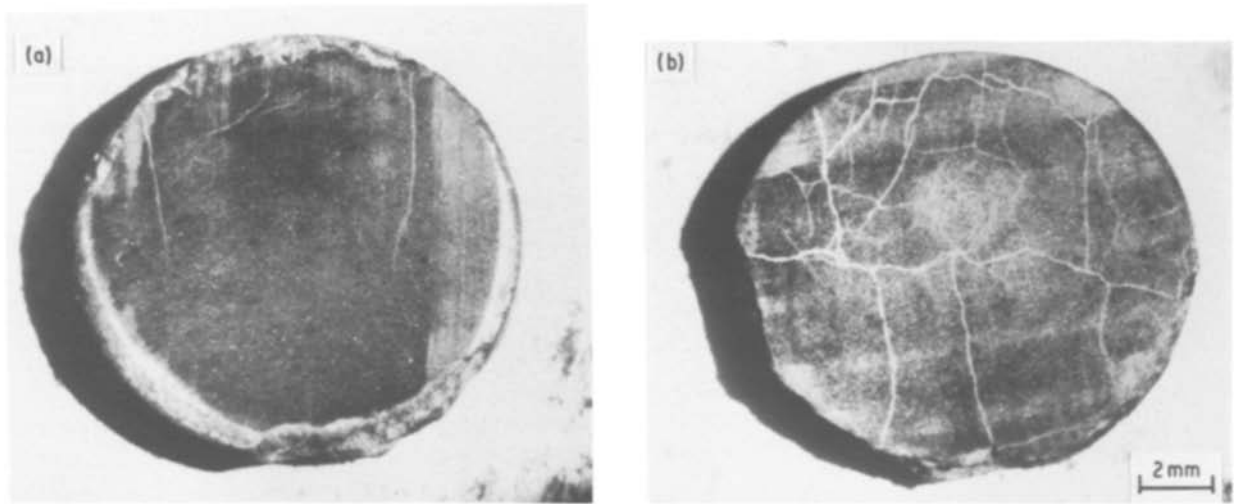
Figure 2 Section views of the polished front (a) and bottom (b) surfaces of compacted coarse c-BN powder (40 to 60 μm grade). ×6.3.

in this figure show the polished front (a) and bottom (b) surfaces. The cracks in the c-BN compacts seem to be partly caused by the high residual stress in the compacts and partly by the abrupt volume expansion associated with the rarefaction wave. The larger number of cracks in the bottom surface than in the front surface, as seen in Fig. 2, seems to be evidence of the effects of the strong rarefaction wave that is associated with the intense radial shock wave generating from the outer part of the bottom region as predicted by the simulation [9].

3.1. Density and microhardness

The densities and Vicker's microhardness values of the compacted c-BN samples are shown in Fig. 3. This reveals a strong dependency of the density and microhardness on the grain size of the starting c-BN powders. Percentages in parentheses in this figure indicate relative densities calculated using the theoretical density of c-BN. X-ray diffraction showed that a trace of
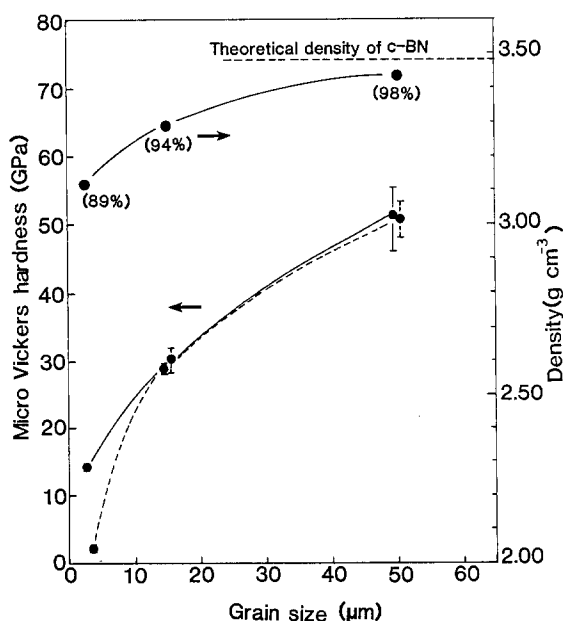
Figure 3 Density and Vicker's microhardness of c-BN compacts. 2 to 4 μm, 10 to 20 μm and 40 to 60 μm grade powders are represented by 3 μm, 15 μm and 50 μm in this figure, respectively. (——) front, (– – –) bottom.

the c-BN in the compacts produced from 10 to 20 μm and 40 to 60 μm grade c-BN powders was transformed to a turbostratic BN (t-BN) [11], and that a part of the c-BN in the compacted fine c-BN powder (2 to 4 μm grade) was converted into t-BN and graphite-like BN (g-BN) by the shock treatments. Thus, the relative densities in Fig. 3 contain some error, especially in the compacts obtained from 2 to 4 μm grade powder.

From the X-ray diffraction, it is seen that the decrease in the density of the compacted c-BN samples with the decrease in grain size of the starting c-BN powders is apparently caused by the conversion of the c-BN to low density forms such as t-BN and g-BN after shock compression, rather than the difficulty in the densification of fine grained powder by a shock wave. Also, this conversion is undoubtedly responsible for the marked reduction in the microhardness of the c-BN compacts with the decrease in c-BN grain size.

In the compacts produced from the 2 to 4 μm and 10 to 20 μm grade powders, the micro Vicker's indentations for a 9.8 N load were larger than an apparent particle size of the c-BN powders after shock treatments. On the other hand, in the compacted 40 to 60 μm grade c-BN sample, indentations were somewhat smaller than the apparent c-BN particle size after shock treatment. Thus, the microhardness of this compact was measured on the c-BN particles and on the boundaries between the particles separately. Some indentations in both positions are shown in Fig. 4. Microhardness of the particles was slightly higher than that in the particle boundaries: 53.3 ± 1.4 GPa for the particles and 51.3 ± 3.6 GPa for the boundaries in the front surface, respectively. In Fig. 3, microhardness values in the front and bottom surfaces of the compacted 40 to 60 μm grade powder are represented by the values obtained on the c-BN particle boundaries. The average microhardness values in the front and bottom surfaces of this compact, 51.3 and 50.6 GPa, are almost equivalent to those for statically synthesized polycrystalline c-BN compacts [4]. This indicates that extensive interparticle bonding has been successfully produced in the compacted coarse c-BN (40 to 60 μm grade) following the densification of the powder in the shock-compaction process. The
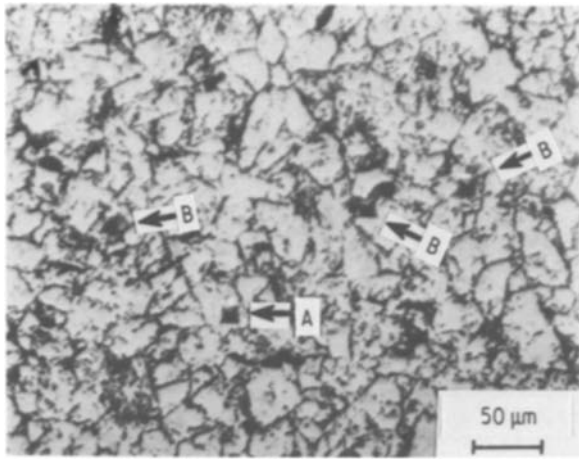
Figure 4 Micro Vicker's indentations in compacted 40 to 60 µm grade c-BN powder. (A) and (B) indicate indentations in the c-BN particles and the particle boundaries, respectively.

difference in the microhardness values of the front and bottom surfaces of the compacted 2 to 4 µm grade c-BN powder is apparently due to the difference in the pressure and temperature histories in both regions during and after shock compression.

3.2. Lattice strain and crystallite size

In general, ceramic powders can be densified by intense particle fracture and plastic deformation under shock compression. As reported in shock-treated ceramic materials [7, 12], plastic deformation in particles during densification usually results in a significant increase of lattice strain in the recovered materials. The residual lattice strain and the crystallite size in the recovered c-BN compacts are shown in Fig. 5 and Table II. Relatively small lattice strain values in the compacted c-BN samples compared to those in shock-treated ceramic powders [12–14] suggest that the c-BN powders are densified by particle
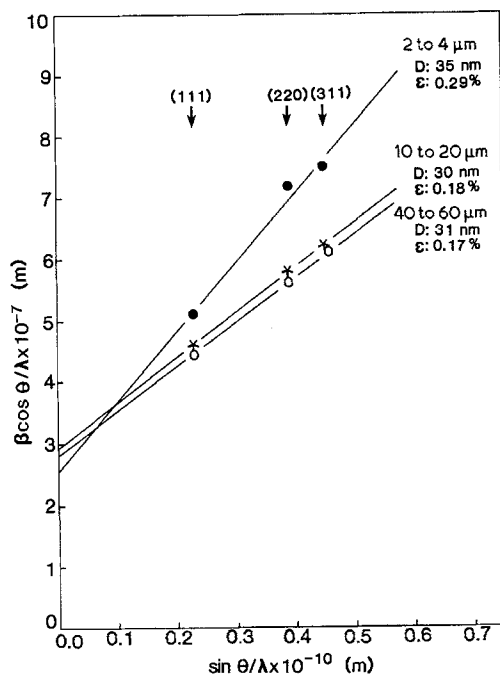
Figure 5 Hall-Williamson plots of X-ray line-broadening analysis. X-ray diffraction patterns were taken using the polished front surfaces of the recovered c-BN compacts. D: crystallite size, E: lattice strain.

TABLE II Lattice strain and crystallite size of compacted c-BN powders

Grain size	Lattice strain (%)		Crystallite size (nm)	
	Front	Bottom	Front	Bottom
2 to 4 µm grade	0.29	0.26	36	32
10 to 20 µm grade	0.19	0.19	30	33
40 to 60 µm grade	0.17	0.14	31	31

fracture. However, scanning electron micrographs of the fracture surfaces of the compacts show that apparent particle sizes of the c-BN after the shock treatments were reduced to about half of the initial grain sizes. Therefore, it is reasonable to conclude that the fine and coarse c-BN powders were densified mainly by plastic deformation rather than by particle fracture, and that the low lattice strain values in the recovered compacts are due to the annealing effects at a high temperature during shock compression and in a part of the pressure release process where the c-BN structure is stable. The lattice strain values, slightly larger in the compacted fine c-BN powder (2 to 4 µm grade) than in the compacted coarse powders (10 to 20 µm and 40 to 60 µm grade) (Fig. 5), seem to be caused by a large plastic deformation in the fine grained powder during densification. This is consistent with the results of dynamically compacted fine and coarse alumina powders by Prümmer and Ziegler [13].

The crystallite size of the compacted c-BN samples was independent of the grain size of the starting c-BN powders (Table II). This suggests that heavily deformed c-BN particles were annealed and then recrystallized into 30 to 35 nm crystallites during shock compression, and not after release of the shock pressure, because c-BN is a stable phase of BN at high pressures. As reported in some shock-compacted ceramic powders, the residual strain and crystallite size are sensitive to temperatures during and after shock compression as well as to the level of shock pressure [12, 14, 15]. In the shock treatment fixture used in this experiment, there is a large difference in temperatures in the front and bottom regions within the powder compacts during and after shock compression [9]. It is, therefore, supposed that the residual strain and crystallite size in both regions of each c-BN compact may be significantly different. However, there is in fact no appreciable difference in the lattice strain and crystallite size in both surfaces of the compacts as seen in Table II. This seems to be caused by the fact that the annealing effects of the deformed c-BN particles can be expected to occur only for an extremely short duration of about 1 µsec, corresponding to the duration of the shock pressure and the part of the pressure release process where c-BN is stable. Thus, the independence of the residual lattice strain on the position within the powder compacts obtained is not inconsistent with the temperature distribution and history during the shock-compaction process within the powders predicted by the simulation [9]. This phenomenon seems to be a unique feature in dynamic compaction of this material.

3.3. Microstructure of c-BN compacts

Typical microstructures of the fracture surfaces in the
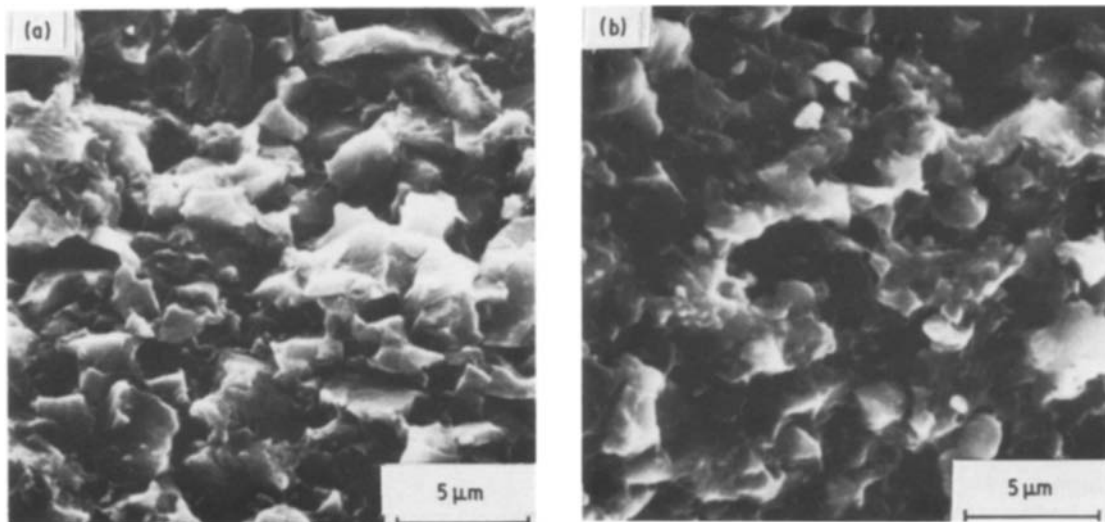
Figure 6 Scanning electron micrographs of a fracture surface of the compacted 2 to 4 μm grade c-BN powder: (a) front region, (b) bottom region.

front (a) and bottom (b) regions of the c-BN compacts produced from the 2 to 4, 10 to 20 and 40 to 60 μm grade powders are shown in Figs 6, 7 and 8. The front region of the compacted 2 to 4 μm grade powder exhibited relatively porous microstructure and mostly intergranular fractures (Fig. 6). Some of the pores in Fig. 6a seem to be remnants of grains which are pulled out at fracturing, which indicate weak interparticle bonding due to the conversion of the c-BN to low density forms, as indicated by X-ray diffraction. With the increase in grain size of the starting c-BN powder from 2 to 4 μm to 10 to 20 μm and 40 to 60 μm, fracture morphology of the resulting compacts gradually changed from intergranular to transgranular fracture in both front and bottom regions, as seen in Figs 6 to 8. Predominance of the transgranular fracture in the c-BN compacts obtained from the 10 to 20 and 40 to 60 μm grade powders is evidence of the development of substantial interparticle bonding during the shock-compaction process. The change in the fracture morphology with the c-BN grain size is very consistent with the phenomenon of the increase in microhardness with the increase in grain size.

Optical micrographs of the polished front surfaces

of three c-BN compacts produced from 2 to 4, 10 to 20 and 40 to 60 μm grade powders are shown in Fig. 9. This clearly shows the difference in the amount of interparticle bonding developed in these compacts. The dark gray regions in the photographs (Fig. 9) were probably made by pulling out of fine grains during polishing. These fine grain regions seem to correspond to the weakly bonded regions where fine c-BN grains, produced during the static powder compaction prior to the shock compaction and during the shock densification, might have been converted into low density forms resulting in friable regions. On the other hand, the bright regions in the photographs correspond to polished c-BN secondary particles. Fig. 9 shows that the size and the number of bright regions in the three c-BN compacts increased markedly with the increase in grain size of the starting powder. In the compact obtained from the 40 to 60 μm grade powder, it can be seen that c-BN particles bonded successfully to each other with a part of each particle. This is also evidence of the substantial interparticle bonding formed in the compact. In the compacted 10 to 20 μm grade powder, interparticle bonding was locally observed but limited by the undesirable
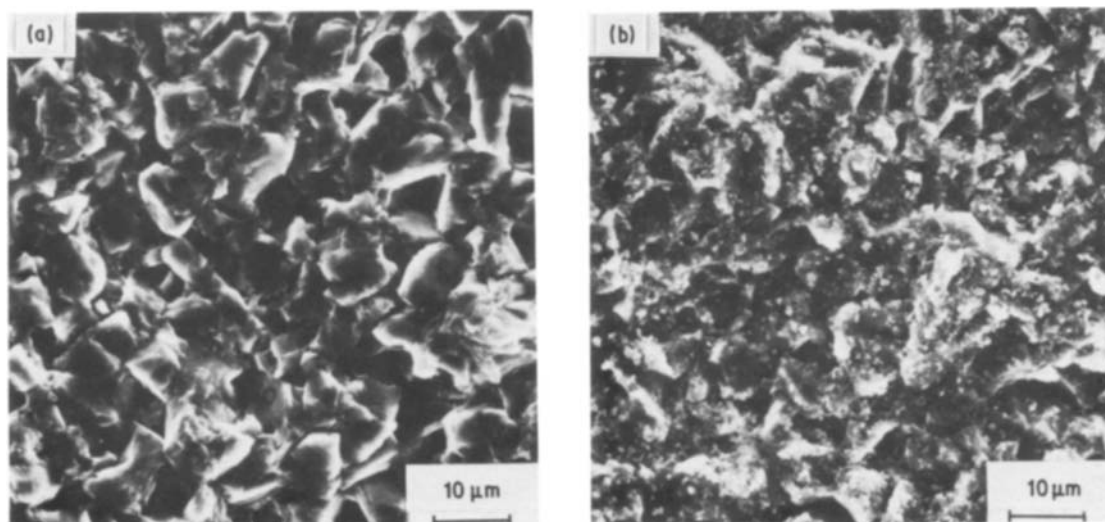
Figure 7 Scanning electron micrographs of a fracture surface of the compacted 10 to 20 μm grade c-BN powder: (a) front region, (b) bottom region.

1131
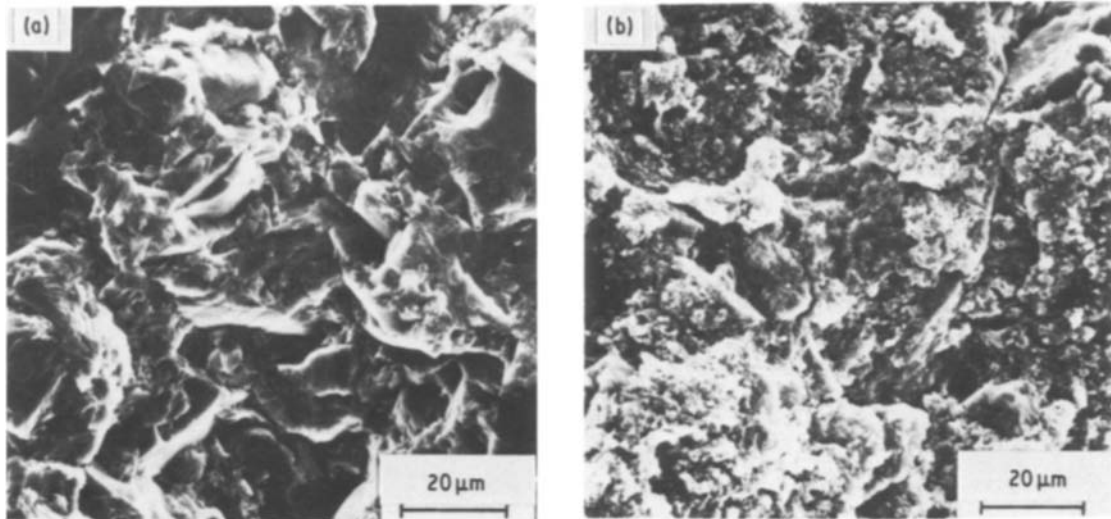
Figure 8 Scanning electron micrographs of a fracture surface of the compacted 40 to 60 μm c-BN powder: (a) front region, (b) bottom region.

conversion of the c-BN to low density forms. Fig. 9 shows that this conversion took place preferentially on the particle surfaces of c-BN (grain boundaries in the compacts).

In the static high pressure sintering of diamond powders, it is also pointed out that graphitization of the diamond occurs preferentially on the surfaces of the diamond grains during sintering [3, 16]. Thus, the surface transformation from a high pressure phase to a low density form that occurs during the consolidation process seems to be a major problem in the sintering of a high pressure modification such as c-BN and diamond. Such a transformation results in a signifi-

cant degradation of the mechanical properties of the resulting compacts.

3.4. Shock consolidation of c-BN powders

Assuming that the Hugoniot of a material is independent of particle size, it can be believed that an increase in the total internal energy of powder compacts consisting of particles with different sizes should be the same for equal initial packing densities as a given shock pressure. In the shock compaction of porous materials, most of the energy has been assumed to be concentrated at particle surfaces as heat during shock compression [17–19]. This heterogeneous heat generation in dynamically compacted powder materials is mainly caused by frictional rubbing and shock compression of gas in the pores during densification [19, 20].

Roman *et al.* [21] studied the effects of powder particle size on shock compaction using tungsten powders with different particle sizes. They found that in the coarse grained powder compact, intense plastic flow took place at grain boundaries and that interparticle bonding developed, while little plastic flow took place and limited self-bonding developed in the shock-compacted fine grained powder. They explained the
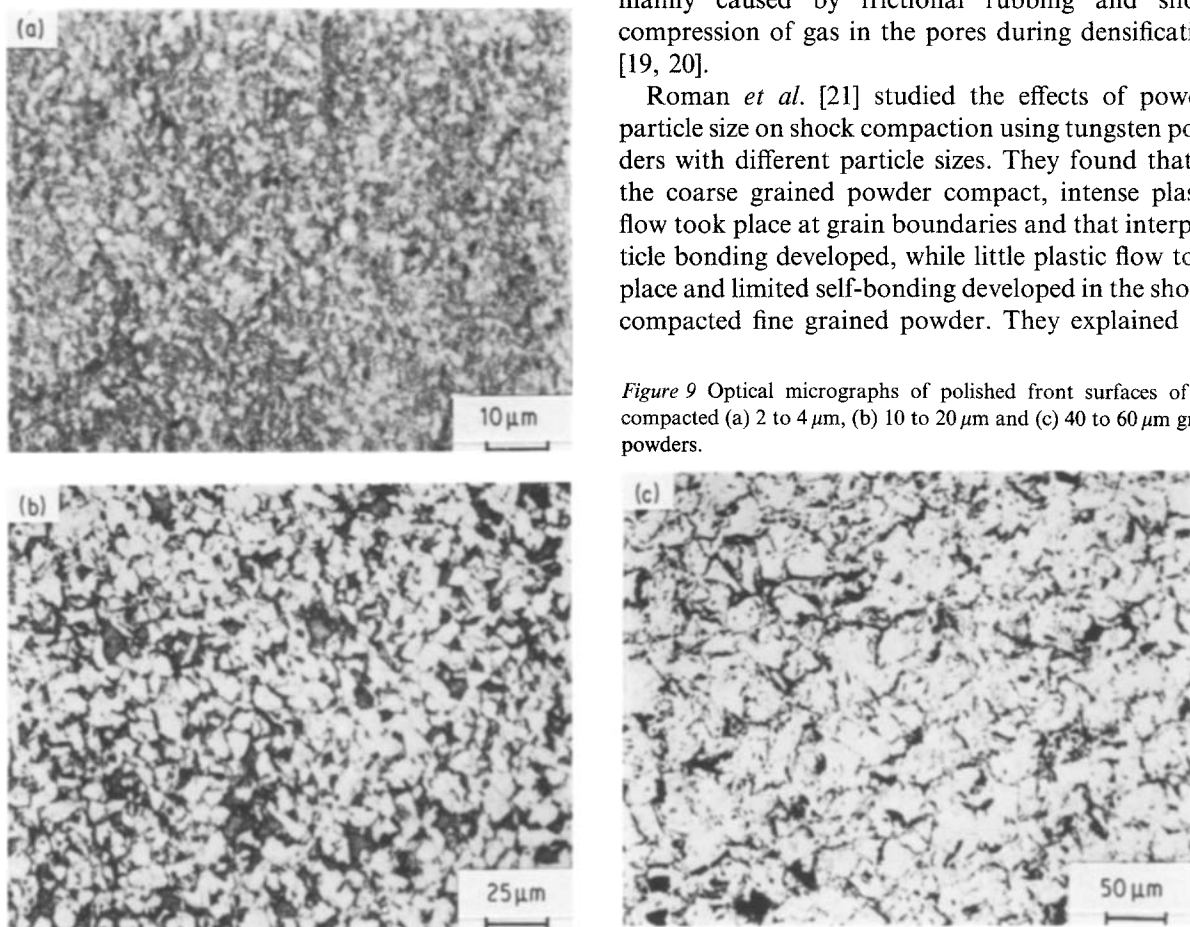
Figure 9 Optical micrographs of polished front surfaces of the compacted (a) 2 to 4 μm, (b) 10 to 20 μm and (c) 40 to 60 μm grade powders.

results by considering the difference in energy distribution in powder compacts due to the different particle sizes. Because of the number of particle contacts per unit volume and the size of the contacts in each powder compact, the temperature at contact surfaces should increase significantly with the increase in particle size of the starting material. Consequently, very fine powder results in a uniform energy distribution over the volume, while coarse grained powder results in a significant energy concentration on the contact surfaces behind the shock front. This dependence of the surface temperature on grain size agrees well with the consideration proposed by Gourdin [22]. Roman et al. [21] suggested that such a high temperature rise at the contact surfaces behind the shock front acted as an important factor in shock compaction of powder materials and enabled the development of the interparticle bonding during the shock-compaction process.

Fine grain structure along the particle boundaries in the bottom region of the compacted 10 to 20 μm grade c-BN powder (Fig. 7b) seems to be evidence of a high temperature rise at the contact surface behind the shock front. Moreover, the amount of the fine grain structure increased with the increase in grain size of the starting c-BN powder from 10 to 20 μm to 40 to 60 μm (Figs 7b and 8b), while there was no such fine grain structure in the compacted fine grained c-BN powder (2 to 4 μm grade) (Fig. 6b). This indicates that the temperature at the contact surfaces in the powder compacts in fact increased with the grain size of the c-BN. The fine grain structure is possibly formed by the recrystallization of heavily deformed regions between grains at high temperature, or even by solidification of the liquid phase of the BN produced at a high temperature at the contact surfaces by considering the pressure–temperature phase diagram of BN [23, 24].

On the other hand, in the bottom region of the compacted fine c-BN powder (2 to 4 μm grade) (Fig. 6b), no fine grain structure was observed, indicating that the temperature at the contact surfaces was significantly lower than that in the compacted coarse c-BN powders. It is therefore considered that the marked difference in the microstructures of the c-BN compacts produced in this work (Figs 6 to 8) is caused by the difference in the energy distribution in the powder compacts due to the different c-BN grain sizes, even though an increase in the internal energy accompanied by the shock compression is the same at a given shock pressure.

The temperature at grain boundaries in the c-BN powder compacts should be quickly decreased by heat transfer to the grain interiors in order to prevent the conversion of the c-BN to low density forms after the release of the shock pressure. Critical particle size of the c-BN powder for the thermal equilibrium in powder compacts during shock compression is estimated to be about 25 μm [15]. Therefore, considering the decrease in grain size of the starting c-BN powder during the static powder compaction and during the shock densification into about half that of the initial grain size, the localized high temperature could be reduced during shock compression even in the compacted coarse c-BN powder (40 to 60 μm grade). This is supported by the fact that only a trace of the c-BN converted into low density forms in the compacted coarse powders (10 to 20 and 40 to 60 μm grade). Furthermore, the absence of g-BN in these compacts suggests that the recrystallization or solidification mentioned above has been accomplished before release of the shock pressure.

Formation of a small amount of g-BN was detected only in the compacted fine grained c-BN powder (2 to 4 μm). This g-BN formation seems to be related to the nature of the surface transformation of c-BN to low density forms, rather than a high residual temperature in this compact because the residual temperatures in the c-BN compacts should be the same. The transformation of c-BN to low density forms at a high temperature under ambient pressure is relative to the crystallite size of c-BN, but not to the apparent particle size. X-ray line-broadening analysis showed that there is no significant difference in the crystallite sizes of the c-BN compacts obtained from different grain sizes (Table II). Therefore, it is concluded that the different conversion behaviour of c-BN to low density form in the recovered compacts resulted from the difference in the degree of the self-bonding between the crystallites that developed in these compacts during the shock-compaction process. The results obtained in this work show that in the coarse c-BN powder compact, consolidation of the powder can be substantially enhanced by the high temperature rise at grain boundaries during shock compression, and that the enhanced consolidation prevents undesirable conversion of the c-BN to low density forms after release of the shock pressure, preserving good mechanical properties of the compacted c-BN powder.

4. Conclusions

The density and microhardness of the shock-compacted c-BN powders are strongly dependent upon the grain size of the starting c-BN powder. Well sintered c-BN compact with 98% of the theoretical density and microhardness of 51.3 GPa can be produced from the coarse c-BN powder (40 to 60 μm grade) by a shock compaction technique. The degree of the transformation of c-BN to low density forms after release of the shock pressure increases with the decrease in initial c-BN grain size. This conversion has significant effects on the density, microhardness and microstructure of the resulting compacts.

In the coarse c-BN powder compact, the consolidation can be enhanced by the high temperature rise at grain boundaries during shock compression. This enhanced consolidation consequently prevents undesirable conversion of the c-BN to low density forms at a residual temperature, preserving good mechanical properties of the c-BN compact. Therefore, in the shock compaction of c-BN, coarse powder is desirable as the starting material in order to produce a well-consolidated compact.

References

1. R. C. DEVRIES, "Cubic Boron Nitride: Handbook of Properties", GE Technical Report No. 72-CRD 178, GE R &

D, New York, (1972).

2. H. D. STROMBERG and D. R. STEPHENS, *Ceram. Bull.* **43** (1970) 1030.
3. N. SUZUKI, A. NAKAUE and O. OKUMA, *J. Jpn High Press. Inst.* **11** (1974) 301.
4. M. WAKATSUKI, K. ICHINOSE and T. AOKI, *Mater. Res. Bull.* **7** (1972) 999.
5. O. R. BERGMAN and J. BARRINGTON, *J. Amer. Ceram. Soc.* **49** (1966) 502.
6. C. L. HOENIG and C. S. YUST, *Ceram. Bull.* **60** (1981) 1590.
7. T. AKASHI, V. LOTRICH, A. SAWAOKA and E. K. BEAUCHAMP, *J. Amer. Ceram. Soc.* **68** (1985) C-322.
8. T. AKASHI and A. B. SAWAOKA, *ibid.* **69** (1986) C-78.
9. F. R. NORWOOD, R. A. GRAHAM and A. SAWA-OKA, to be published in the Proceedings of the 4th APS Topical Conference on Shock Waves in Condensed Matter, Spokane, Washington, USA, July 22–25, 1985.
10. H. P. KLUG and L. E. ALEXANBER, "X-ray Diffraction Procedures", (John Wiley, New York, 1975) p. 491.
11. J. THOMAS, Jr, N. E. WESTON and T. E. O'CONNOR, *J. Amer. Chem. Soc.* **84** (1963) 4619.
12. R. A. GRAHAM, B. MOROSIN, E. L. VENTURINI, and W. F. HAMMETTER, "Emergent Process Methods for High-Technology Ceramics" edited by R. F. Davis, H. Palmour III and R. L. Porter, Material Science Research, Vol. 17 (Plenum Press, New York, 1985) p. 718.
13. R. PRÜMMER and G. ZIEGLER, *Powder Metall. Int.* **9** (1977) 73.
14. B. MOROSIN and R. A. GRAHAM, *Mater. Sci. Engr.* **66** (1984) 73.
15. K. KONDO, S. SOGA, A. SAWAOKA and M. ARAKI, *J. Mater. Sci.* **20** (1985) 1033.
16. M. AKAISHI, H. KANDA, Y. SATO, N. SETAKA, O. OHSAWA and O. FUKUNAGA, *ibid.* **17** (1982) 193.
17. D. G. MORRIS, *Metal Sci.* **15** (1981) 116.
18. D. RAYBOULD, *J. Mater. Sci.* **16** (1981) 589.
19. D. G. MORRIS, *Mater. Sci. Engr.* **57** (1983) 187.
20. V. F. LOTRICH, T. AKASHI and A. SAWAOKA, to be published in the Proceedings of the 4th APS Topical Conference on Shock Waves in Condensed Matter, Spokane, Washington, USA, July 22–25, 1985.
21. O. V. ROMAN, U. F. NESTERENKO and I. M. PIKUS, *Combustion, Explosion and Shock Waves* **15** (1980) 644.
22. W. H. GOURDIN, *J. Appl. Phys.* **55** (1984) 172.
23. F. P. BUNDY and R. H. WENTORF Jr, *J. Chem. Phys.* **38** (1963) 1144.
24. J. A. VAN VECHTEN, *Phys. Rev. B* **7** (1973) 1479.